phoric oligosilane segments, each of which is characterized by a single intense absorption and emission contribution of the σ–σ^* type at an energy dictated by its length and exact geometry. The similarity of the two assemblies accounts for the similarity of the observed absorption spectra.

The fundamental difference between the two cases is the absence of covalent links between some of the individual chromophoric segments in the case of the hexadecasilane model. This makes little difference in absorption, but has two important consequences that are potentially important for emission spectra. However, their effects compensate: the absence of the links limits the extremely fast intersegment energy transfer known from the polymer to a range of no more than 16 silicon atoms, and it greatly enhances conformational mobility within such groups of 16 silicon atoms in media of low viscosity.

In both cases, emission from a room-temperature solution occurs primarily but not exclusively from about 16-silicon chromophoric segments of the lowest excitation energy (presumably all-trans), and the cutting of the polysilane backbone into 16-silicon pieces thus has almost no effect. In the polymer, excitation in any chromophoric segment is largely transferred to the lowest energy chromophores by energy transfer over considerable distances along the backbone with some emission occurring in competition, resulting in a weak excitation energy dependence of the fluorescence shape. In hexadecasilane, the excitation of any chromophoric segment is transformed into excitation of the lowest energy chromophores by an adiabatic distortion of the molecular geometry of the now freely mobile 16-silicon segments, with some emission occurring in competition, resulting in the same weak excitation energy dependence of the fluorescence shape.

In a high-viscosity medium, such as a low-temperature glass, the superficial nature of the near identity of the fluorescence properties of the high polymer and the hexadecasilane is revealed. Now, the absence of long-range energy transfer can no longer be compensated by conformational mobility, and the spectrum of the hexadecasilane changes dramatically.

Individual noncommunicating conformers now act independently, and three of them (A, B, and C) dominate the spectra. Their structures are not known, but they are clearly distinct from each other and from the presumably all-trans low-energy conformer or conformers that dominated room-temperature emission.

Even at concentrations as low as 5×10^{-6} M, and more so at higher concentrations, $Si_{16}Me_{34}$ aggregates when its solution in 3-methylpentane is cooled rapidly to 77 K, and the picture is complicated further. The structure of the aggregate, termed dimer for simplicity, is not known, but it is likely to be a very loose, structurally disorganized collection of weakly communicating hexadecasilane molecules transferring energy to an emissive center that is probably similar to A.

Slow cooling and the use of higher concentrations results in the formation of microcrystals of a solid. Its absorption and emission properties fit expectations for a crystal that contains parallel chains of hexadecasilane molecules.

Acknowledgment. This work was supported by AFOSR Grant Nos. 87-0001, 89-0004, and 91-0032. We thank Dr. Robert D. Miller (IBM Almaden Research Center) for a kind gift of poly(methylpropylsilane) and Dr. Stephen J. Atherton for his help in the fluorescence lifetime measurements at the Center for Fast Kinetics Research, jointly supported by the Biotechnology Branch of the Division of Research Resources of the National Institutes of Health and the University of Texas at Austin.

Photoreactivity of the Conjugate Bases of Two Aromatic Ketones: Photochemistry of the Enolates of α,α-Diphenylacetophenone and Deoxybenzoin

Shiyamalie R. Ruberu and Marye Anne Fox*

Contribution from the Department of Chemistry, University of Texas at Austin, Austin, Texas 78712. *Received January 6, 1992*

Abstract: Photoexcitation of the enolate anion of deoxybenzoin (**4**) induces geomeric isomerization, as evidenced by ground state bleaching and formation of a metastable isomer. In aerated THF, the enolate of α,α-diphenylacetophenone **5** reacts by electron transfer to the excited triplet state of its thermal autoxidation product benzophenone. The calculated geometries of **4** and **5** (AM-1) correlate well with those found by solution and solid-state NMR spectroscopy, with enolate **4** existing as the more stable *Z*-isomer and enolate **5** in a twisted, locked geometry. The effect of ion pairing on the absorption spectra and the redox potentials of enolates **4** and **5** are discussed.

Introduction

While it is well-known that photoexcitation of organic carbanions and oxyanions[1-3] often leads to different products than are formed from the excited states of their neutral precursors, the scope of such reactions and their applicability as efficient organic transformations have yet to be established. In particular, the structural features which cause the contrasting photoreactivity of neutral ketones and their conjugate base enolate anions[4-8] are unclear.

---

(1) Tolbert, L. M. *Acc. Chem. Res.* **1986**, *19*, 268.

(2) Tolbert, L. M. *Org. Photochem.* **1983**, *6*, 177.

(3) Fox, M. A. *Chem. Rev.* **1979**, *79*, 253.

(4) Scamehorn, R. G.; Bunnett, J. F. *J. Org. Chem.* **1977**, *42*, 1457.

(5) Rossi, R. A.; Bunnett, J. F. *J. Org. Chem.* **1973**, *38*, 1407.

(6) van Tamelen, E. E.; Schwartz, J.; Brauman, J. I. *J. Am. Chem. Soc.* **1970**, *92*, 5798.

(7) Padwa, A.; Dehm, D.; Oine, T.; Lee, G. A. *J. Am. Chem. Soc.* **1975**, *97*, 1837.

(8) Westmore, R. W.; Schaefer, H. F.; Hiberty, P. C.; Brauman, J. I. *J. Am. Chem. Soc.* **1980**, *102*, 5470.

0002-7863/92/1514-6310$03.00/0

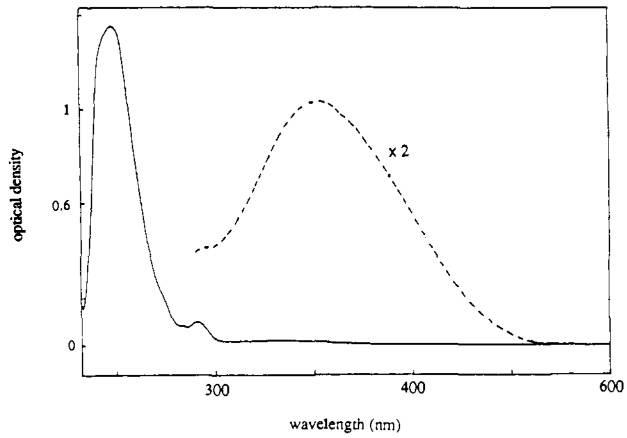

Figure 1. Absorption spectra of **5** (--) as a sodium enolate (1 mM) and its neutral precursor (0.5 mM) (—) at 25 °C in dry degassed THF.

White and co-workers[9,10] have shown that the photolysis of a trienolate anion **1** diverges markedly from that of the corresponding neutral β-ketoester, resulting in an efficient cyclization of the anion, eq 1. In order to determine whether White's photocyclization is general for simple conjugated enolates, we have examined the photoreactions of several other conjugated trienenolates which bear either a very similar carbon skeleton, e.g., the enolate of β-ionone (**2**), or which incorporate one of the double bonds within an aromatic ring, e.g., the enolates of benzalacetone (**3**), deoxybenzoin (**4**), and α,α-diphenylacetophenone (**5**). Of these anions, only **2** shows a substantial yield of cyclization product, producing, however, a pyran rather than a carbocyclic product.[11] In seeking to better understand the factors influencing the divergent photochemical behavior of these conjugated enolates, we have investigated the photoreactivity of enolates **2**–**5**, with particular emphasis on the structurally similar aromatic enolate anions **4** and **5**.

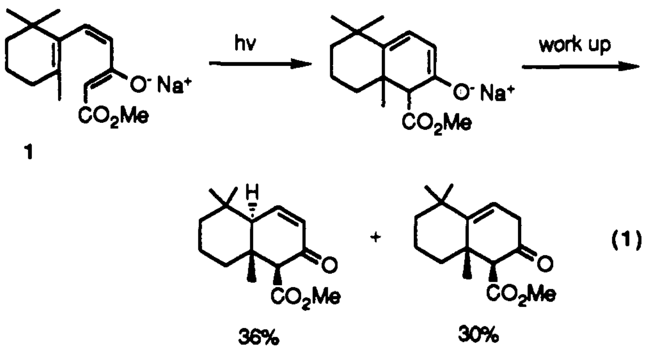

(1)

Results and Discussion

Steady State Photolysis: Product Studies. The sodium enolates **2**–**5** were generated by treatment with a slight excess of sodium hydride in tetrahydrofuran (THF). In all cases, a red-shifted absorption band characteristic of the enolate accompanied the deprotonation, Figure 1, making selective excitation of the enolates possible.

Upon photoexcitation, followed by neutralization, **2** was found to have cyclized to an α-pyran rather than to the isomeric carbocyclization product. γ-Ionone, resulting from a transformation which has effected a net [1,5]-hydrogen shift in the excited singlet state, is also a major side product, eq 2.[11] Geometric isomerization is the dominant photoreaction of the conjugated enolate anion of benzalacetone (**3**), eq 3, producing a photostationary state with a Z/E ratio of 1.63. At wavelengths >300 nm, where the enolate anions **4** and **5** can be selectively excited,[8,29] Figure 1, none of the usual Norrish type I cleavage products formed from n,π^* excitation of the neutral ketone could be observed.[30] No stable cyclization photoproducts could be observed with **4**, eq 4, in contrast to the well-known photoreactivity of stilbene, a hydrocarbon possessing a similar carbon skeleton,[12] eq 5.

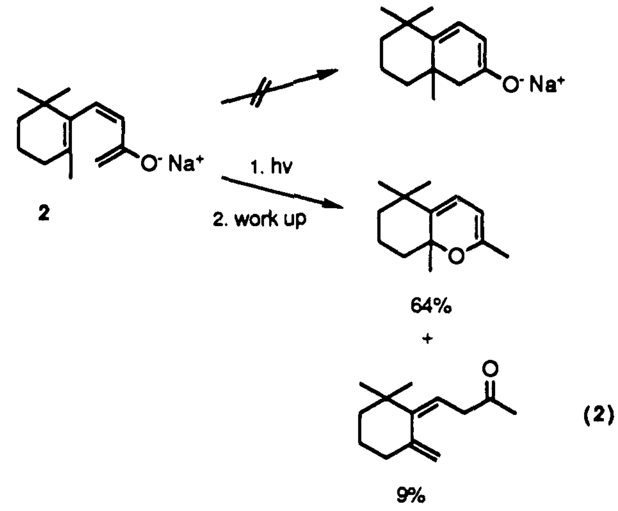

(2)

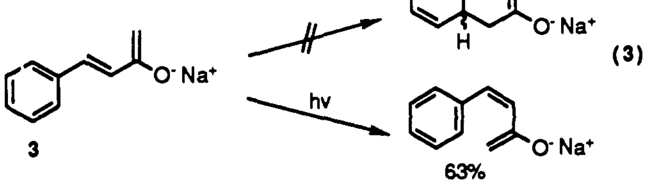

(3)

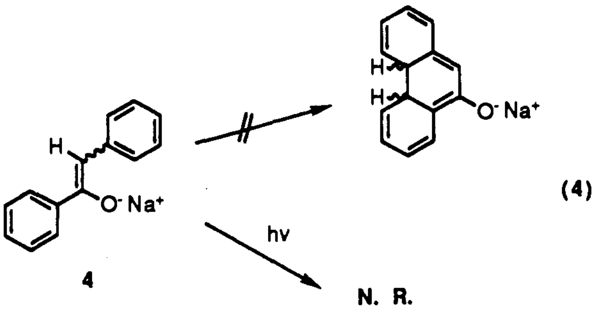

(4)

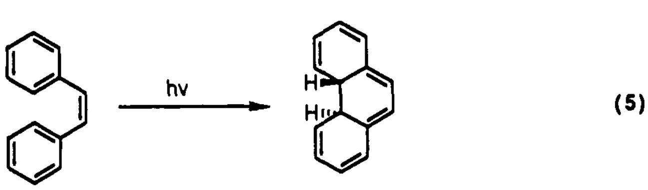

(5)

In anion **5**, where geometric isomerization simply regenerates the starting material, no cyclization product can be isolated, although a photoproduct is observed in the presence of even traces of oxygen, eq 6. The enhanced electron density in enolate **5** appears to be critical in blocking the photocyclization, since van Ginkel, Cornelisse, and Lodder[13] have recently reported that the enolacetates derived from substituted **5** do, in fact, cyclize in reasonable yield. We have therefore undertaken a more detailed physical characterization of anions **4** and **5** with special emphasis on factors influencing geometric isomerization.

---

(9) White, J. D.; Skeean, R. W. *J. Am. Chem. Soc.* **1978**, *100*, 6296.

(10) White, J. D.; Skeean, R. W.; Trammell, G. L. *J. Org. Chem.* **1985**, *50*, 1939.

(11) van Wageningen, A.; Cerfontain, H.; Geenevasen, J. A. *J. Chem. Soc., Perkin Trans. 2* **1975**, 1283.

(12) Saltiel, J.; D'Agostino, J.; Megarity, E. D.; Metts, L.; Neuberger, K. R.; Wrighton, M.; Zafiriou, O. C. In *Organic Photochemistry*; Chapman, O. L., Ed.; Dekker: NY, 1973; Vol. 3, p 1.

(13) van Ginkel, F. I. M.; Cornelisse, J.; Lodder, G. *J. Am. Chem. Soc.* **1991**, *113*, 4261.

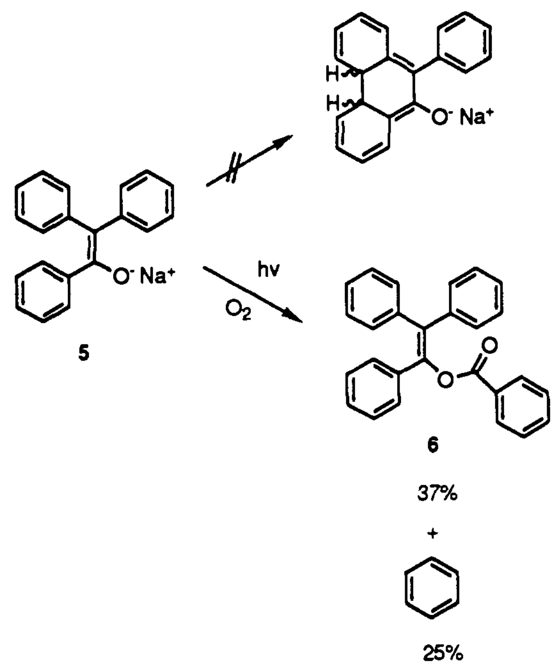

(6)

Generation and Spectral Characteristics of Anions 4 and 5. That anions **4** and **5** are generated quantitatively by treatment of the corresponding ketones with a slight excess of either sodium hydride or lithium diisopropylamide in THF was demonstrated by analyzing the products obtained upon quenching the reaction mixture with D_2O or MeI. The free anions in solution were generated from the sodium enolate by adding a few drops of hexamethylphosphoramide (HMPA) as cosolvent.

The absorption spectra of **4** and **5** are characterized by shifts to longer wavelengths than in their neutral precursors, Table I. Larger shifts are observed as the association between the enolate and its counterion decreases. The shifts observed for anions **4** and **5** (10–100 nm) are smaller than those previously reported for more tightly ion-paired carbanions and oxyanions.[3] Larger bathochromic shifts are seen in anion **4** than **5**, presumably because the former can assume a more planar geometry, thereby permitting charge delocalization and decreasing its association with the countercation. An analogous dependence of the magnitude of the observed spectral shifts on cation radius has been attributed to a difference in a shift of the ion pair equilibrium in the excited state from that in the ground state.[3,14,15]

Anion **4**, as a lithium or sodium salt or free ion, shows weak fluorescence at approximately 450–460 nm at room temperature, with no distinguishable blue shift with increasing cationic radii, in contrast to the observed shifts of emission bands of tightly ion-paired aromatic oxyanions.[16,17] Anion **5** does not emit in solution at room temperature. The nonplanarity and nonrigidity of these anions, together with the possibility of enhanced intersystem crossing, are probably responsible for the observed emission inefficiency.[18]

The oxidation peak potentials of **4** and **5** referenced to an internal standard ferrocene/ferrocenium couple were measured by cyclic voltammetry in THF at 25 °C, Figure 2. Anion **4** showed an irreversible oxidation at −0.73 V, while anion **5** showed a quasi-reversible oxidation at −0.82 V. These values are comparable to those of related enolates (e.g., phenylacetone −0.74 V vs Cp_2Fe) studied by Federlin and co-workers.[19,20]

Table I. Absorption Spectral Maxima for Enolates **4** and **5** and Their Ketone Precursors

	4 λ_{max} (ϵ_{max})	**5** λ_{max} (ϵ_{max})
ketone	323 (126)[30a]	327 (200)[30a]
Li^+ enolate	360 (4023)[b]	344 (5312)[b]
Na^+ enolate	376 (4170)[b]	354 (5417)[b]
free anion	382 (4736)[b]	362 (5920)[b]

[a] Measured in cyclohexane at room temperature. [b] Measured in dry THF at room temperature.

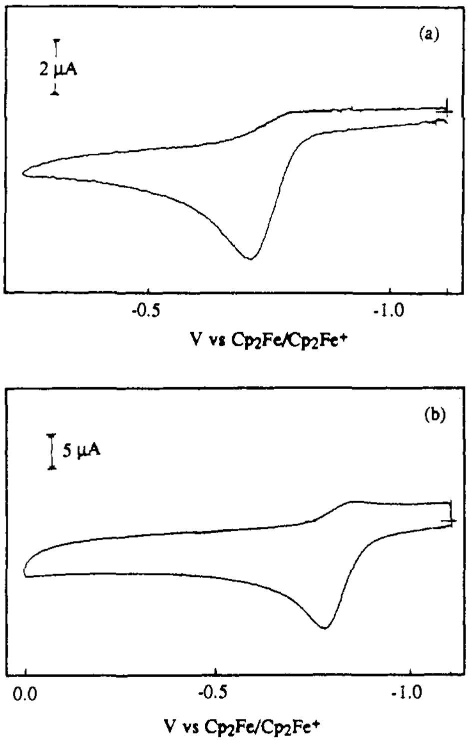

Figure 2. Cyclic voltammograms of (a) **4**, 200 mV/s and (b) **5**, 500 mV/s as TBAP enolates (1 mM) in dearated THF containing 0.3 M $TBAPPF_6$ on Pt at 25 °C. Potentials were recorded against a Cp_2Fe/Cp_2Fe^+ referenced to Ag/AgCl.

Geometries of Anions 4 and 5. A. Solution Phase NMR Spectra.[21] Anion **4** exists in solution as predominantly one geometric isomer. A single vinyl peak (5.6 ppm) is present in the solution phase ^1H NMR spectrum of **4**. Upfield shifts from the corresponding resonances in the neutral are seen for this vinyl proton, H_e, and for the p-ring proton, H_d (67 ppm), indicating appreciable negative charge density, while the smaller chemical shift for the ortho protons, (7.8 ppm) H_a, indicates less charge at those sites.[22] Similarly, in the ^{13}C spectrum, the quaternary carbon C_J (93.9 ppm) has moved upfield, while C_H and C_I (at 125 and 120 ppm, respectively) have moved further downfield. This same charge distribution is obtained in the AM-1 semiempirical MO calculations (see below).

In order to establish whether this anion is the *E*- or *Z*-isomer, the enolate **4** was trapped chemically by an excess of acetic anhydride, producing a single isomeric enol acetate in 97% yield.[23] In this product, the observed chemical shift of the vinyl proton (6.7 ppm/$CDCl_3$) corresponds closely to that expected for the *Z*-geometry.[24]

The solution phase ^{13}C NMR spectrum of anion **5** shows 18 different C atom chemical shifts, indicating a locked conformation

---

(14) Smid, J. In *Ions and Ion Pairs in Organic Reactions*; Szwarc, M., Ed.; Wiley Interscience: New York, 1972; Vol. 1, p 85.

(15) Zaugg, H. E.; Schaefer, A. D. *J. Am. Chem. Soc.* **1965**, *87*, 1857.

(16) Soumillion, J. P.; Vandereecken, P.; Van der Auweraer, M.; De Schryver, F. C.; Schanck, A. *J. Am. Chem. Soc.* **1989**, *111*, 2217.

(17) Velthorst, N. H. *Pure Appl. Chem.* **1979**, *51*, 85.

(18) Bowen, E. J. *Luminescence in Chemistry*; Van Nostrand: Canada, 1968; p 77.

(19) Kern, J. M.; Federlin, P. *Tetrahedron Lett.* **1977**, *10*, 837.21.

(20) Kern, J. M.; Federlin, P. *Tetrahedron* **1978**, *34*, 661.

(21) For positional numbering, see Figure 3.

(22) Such an observation has been reported with other enolate anions where negative charge is allowed to localize freely: Bradamante, S.; Pagani, G. A. *J. Chem. Soc., Perkin Trans. 2* **1986**, 1035.

(23) (a) House, H. O.; Kramar, V. *J. Org. Chem.* **1963**, *28*, 3362; (b) Suzuki, A.; Ohmori, K.; Itoh, M. *Tetrahedron* **1969**, *25*, 3707.

(24) Bach, R. D.; Woodard, R. A.; Anderson, T. J.; Glick, M. D. *J. Org. Chem.* **1982**, *47*, 3707.

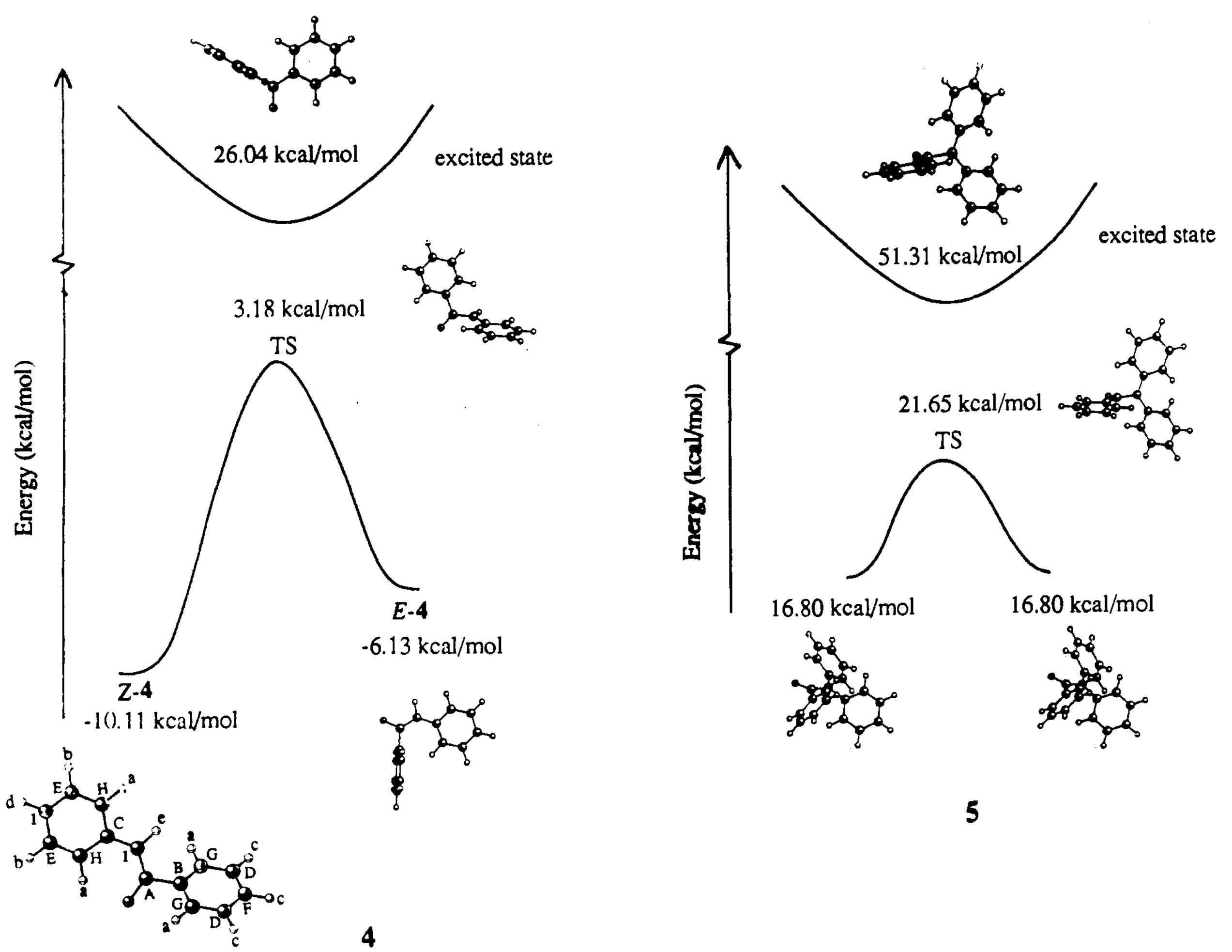

Figure 3. AM-1 calculated energy profiles for optimized geometries and for bond rotation about the enolic double bond in free anions **4** and **5** in the ground and excited states.

with only one phenyl group freely rotating, probably the cross-conjugated ring. The ^1H NMR spectrum shows complex sets of peaks in the region between 6.8 and 7.8 ppm.

B. Solid State NMR Spectra. Solid state NMR spectra of anions **4** and **5** both show the incorporation of THF, presumably as solvent of recrystallization. ^{13}C chemical shift values in the solid samples are almost identical to those observed in solution, except for the C_J in **4**, where a single peak at 94 ppm in solution is resolved into two peaks (94.5 and 98 ppm) in the solid state, indicating the presence of both *E*- and *Z*-isomers in the solid anion.[25] The solid state ^{13}C NMR spectrum of anion **5** exactly matches its solution spectrum.

C. AM-1 Calculations. Figure 3 shows optimized geometries of anions **4** and **5** obtained via semiempirical (AM-1) calculations[26] as well as energy profiles for the ground and lowest singlet excited state surfaces and for bond rotation about the α,β-enolate C=C double bond. Anion **4** is predicted to exist as the more stable *Z*-isomer (favored over the *E*-isomer by ca. 4 kcal/mol) in a nearly planar enolate geometry with the phenyl ring attached to C_B at a dihedral angle of ca. 40°. This twisting, also seen in α-substituted benzyl anions,[21] relieves the nonbonding interactions between the ortho ring hydrogens with atoms or groups α to the carbanionic carbon. For example, although *trans*-stilbene exists in a nearly planar geometry in the solid state or in a supersonic jet, it assumes a 32° twist dihedral angle in the gas phase because of steric interaction of the ortho hydrogens.[27c] The higher energy *E*-isomer of **4** has its phenyl groups twisted 82° and 3°, respectively, out of the plane, thus making **4** less planar than *cis*-stilbene, whose twist angle is only 43°.[27c] To maximize conjugation, the phenyl group at C_B (rather than at C_C) is twisted. Thus, the observed preferential stability of the *Z*-isomer is probably electronic, caused by better conjugation. This energy difference is slightly greater than that seen in the *cis*- and *trans*-stilbenes (~5 kcal/mol)[28] and is roughly consistent with the difference in oxidative peak positions in the cyclic voltammetric oxidations of **4** and **5**. A geometric isomerization of **4** takes the anion to a twisted transition state (TS) with a calculated activation energy of about 13 kcal/mol for the $Z \rightarrow E$ and 9 kcal/mol for the $E \rightarrow Z$ conversions.

The optimized ground state geometry of **5** has all three phenyl rings twisted from the molecular plane to avoid steric crowding. The largest twisting is also seen in the phenyl ring attached to the C-oxygen carbon (52°), with the C-α rings twisted 40° and 24°, respectively. In the excited state anion **5** becomes almost planar, with much smaller twist angles of 0.8°, 26°, and 29° for the phenyl groups than in the corresponding excited state of **4**. Rotation about the $C\alpha$–$C\beta$ carbon–carbon bond in the ground state **5** proceeds with a lower activation energy barrier (4.8 kcal/mol) than in **4** despite the bulky phenyl group. Presumably,

---

(25) Lack of extended planarity in the *E*-isomer should prevent delocalization of negative charge into the benzene ring to some extent, thereby increasing the π charge density on the carbanionic carbon, which would allow C_J to acquire a different chemical shift from the *Z*-isomer. The ratio of the *Z*/*E*-isomers, obtained from integration of these signals, varied from sample to sample, implying that the presence of the *E*-isomer was caused by a matrix effect induced during crystallization rather than by thermodynamic equilibration.

(26) Dewar, M. J. S.; Zoebisch, E. G.; Healy, E. F.; Stewart, J. J. P. *J. Am. Chem. Soc.* **1985**, *107*, 3902.

(27) (a) Champagne, B. B.; Pfanstiel, J. F.; Plusquellic, D. F.; Pratt, D. W.; van Herpen, W. M.; Meerts, W. L. *J. Phys. Chem.* **1990**, *94*, 6. (b) Spangler, L. H.; van Zee, R. D.; Blankespoor, S. C.; Zwier, T. S. *J. Phys. Chem.* **1987**, *91*, 6077. (c) Hohlneicher, G.; Muller, M.; Demmer, M.; Lex, J.; Penn, J. H.; Gan, L.; Loesel, P. D. *J. Am. Chem. Soc.* **1988**, *110*, 4483.

(28) Saltiel, J.; Ganapathy, S.; Werking, C. *J. Phys. Chem.* **1987**, *91*, 2755.

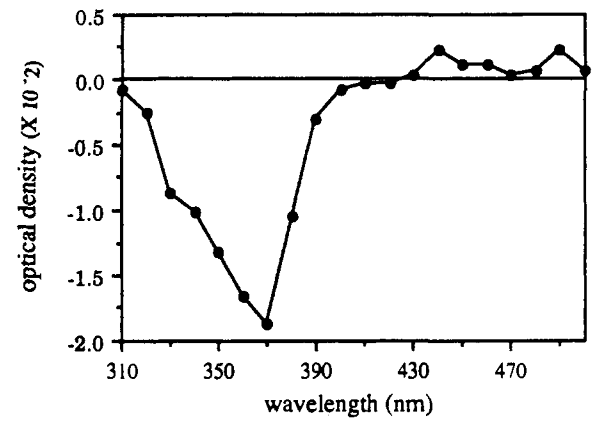

Figure 4. Transient spectrum obtained after 355-nm, 8 ns pulse width excitation of **4** as sodium enolate in freshly distilled THF.

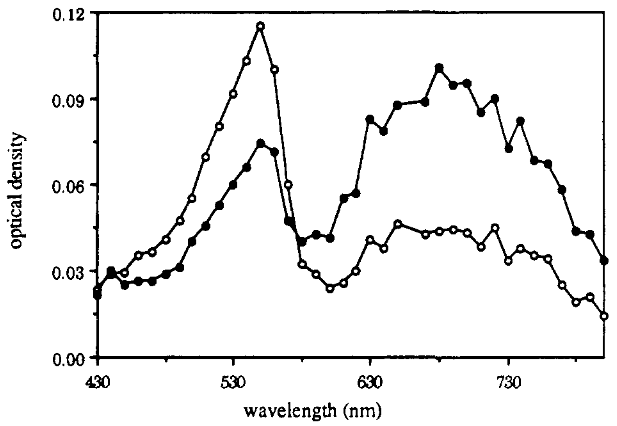

Figure 5. Transient absorption spectra after 355-nm, 8 ns pulse width excitation of **5** in freshly distilled THF. Curves correspond to spectra taken at two delay times after the excitation pulse: –○– 1.22 ms, –●– 9.78 ms.

Scheme I. Photolysis of **5** Sodium Enolate as a 10^{-3} M THF Solution

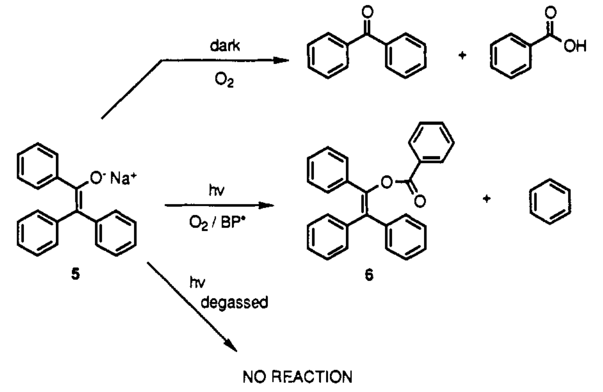

an appreciable twist in the ground state makes it easier for **5** to isomerize.

Steady State and Flash Photolysis of 4 and 5. Although cyclization of **4** analogues to that in *cis*-stilbene[12,28,31] is not observed, twisting of **4** upon photolysis was evident upon flash excitation. Flash photolysis of **4** in degassed and partially aerated THF produced no transient absorptions in the range 400–800 nm with lifetimes longer than 8 ns. However, as shown in Figure 4, a fully reversible bleaching of the ground state was observed. This transient, whose absorption spectrum is very similar to its photochemical precursor, save for the extinction coefficient at the wavelength of maximal bleach, lives for about 14 ms before it quantitatively reverts to ground state **4**. This lifetime is substantially longer than that predicted from the calculated activation energy barrier and an assumed pre-exponential (A factor) typical for analogous systems. Its absorption spectrum is 6 nm blue-shifted (to 700 nm) from the spectrum of the ground state isomer.

Saltiel[28] has pointed out that *trans*-stilbene attains a transoid excited singlet state which decays via a twisted state to give *cis*- and *trans*-stilbene in nearly equal amounts, with the cis isomer then undergoing a geometric isomerization in competition with ring closure. Excitation of anion **4** probably leads to a twisted isomer, possibly reflecting an electronic redistribution within the molecule. Relaxation from this twisted isomer to the starting *Z*-geometry is apparently preferred over cyclization. The lower energy of the excited state of anion **4** may lead to enhanced radiationless decay to a metastable isomer which ultimately relaxes back to the ground state.

Irradiation of a 10^{-3} M solution of **5** in dry, freshly distilled THF partially deaerated by bubbling under N_2 (300–350 nm, low pressure Hg lamps, 4 h) produced the enol ester **6** (37%), together with comparable amounts of benzene (~25%) and benzophenone (BP, 17%).[32] A dark control experiment demonstrated that the latter product arises from a slow thermal autoxidation[33,34] of the anion by dissolved oxygen, Scheme I. In rigorously degassed THF, BP formation is suppressed, and neither the ester nor any other photolysis product could be isolated. Upon addition of BP to the degassed reactant mixture, **6** is produced. The oxygen concentration present in dry air-saturated THF, freshly distilled from BP/Na^+ ketyl to exclude adventitious moisture, produces an adequate steady state concentration of BP for ester formation. The formation of **6** proceeded with consumption of both the thermally produced BP and anion **5**. Selective excitation of **5** at wavelengths $\lambda > 400$ nm (up to 8 h) did not produce **6**, whereas irradiation at shorter wavelengths ($\lambda \geq 300$ nm, medium pressure Hg lamp, into the region where benzophenone is itself excited, 1.5 h) gave **6** in 19% yield.

Flash photolysis of **5** at 355 nm in partially aerated, freshly distilled THF produced two short-lived transient absorptions, at 550 nm and a broader band at 680 nm, Figure 5. In rigorously degassed THF, when BP is absent, neither transient could be observed, indicating that these transients are not formed directly from the anion. When the reaction mixture was saturated with oxygen (conditions under which the thermal reaction produces free BP), the relative intensity of the 550-nm transient absorption increased. Both transients could be trapped by dissolved oxygen, with two discrete apparent quenching rate constants[35] being obtained by a Stern–Volmer analysis. The initial absorption at 550 nm decays simultaneously (within experimental error) with the growth of the second absorption at 680 nm, with a first-order decay rate constant of $5 \pm 2 \times 10^4$ s^{-1} measured at 550 nm. Flash photolysis of BP in THF in the absence of the anion showed the transient at 550 nm, but no peak at 680 nm.

The band at 550 nm is assigned to BP triplet,[36,37] while that at 680 nm is attributed to the Na^+ benzophenone ketyl radical ($BP^{\bullet-}$).[38] Single electron transfer from carbanions[39] or oxyanions[36]

---

(29) Mattay, J. *Syn.* **1989**, 233.

(30) Heine, H.-G.; Hartmann, W.; Kory, D. R.; Magyar, J. G.; Hoyle, C. E.; McVey, J. K.; Lewis, F. D. *J. Org. Chem.* **1974**, *39*, 691.

(31) Saltiel, J.; Sun, Y.-P. In *Photochromism, Molecules and Systems*; Dürr, H., Bouas-Laurent, H., Eds.; Elsevier: Amsterdam, 1990, p 64.

(32) Chemical yields were determined by gas chromatography against a calibrated internal standard (pentadecane) and are based on the consumption of starting material **5**.

(33) Doering, W. v. E.; Haines, R. M. *J. Am. Chem. Soc.* **1954**, *76*, 482.

(34) Gersmann, H. R.; Bickel, A. F. *J. Chem. Soc. B* **1971**, 2230.

(35) Dark interaction of **5** with O_2 produces BP, creating a flux in the concentration of ground state BP and O_2 on which the decay rate measurements are based and producing apparent rate constants which deviate from values reported in literature for these processes in the absence of **5**: Saltiel, J.; Atwater, B. W. *Adv. Photochem.* **1988**, *14*, 25. This discrepancy arises from our inability to simultaneously establish precisely local concentration of the oxygen quencher because of its thermal consumption before the flash excitation.

(36) Bhattacharyya, K.; Das, P. K. *J. Phys. Chem.* **1986**, *90*, 3987.

(37) Devadoss, C.; Fessenden, R. W. *J. Phys. Chem.* **1990**, *94*, 4540.

Scheme II. Proposed Mechanism for the Formation of **6**

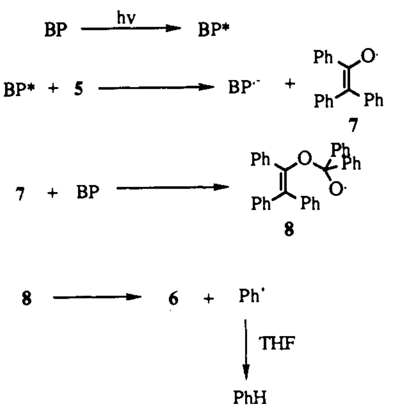

Scheme III. Possible [2 + 2] Cycloaddition Route for **5**

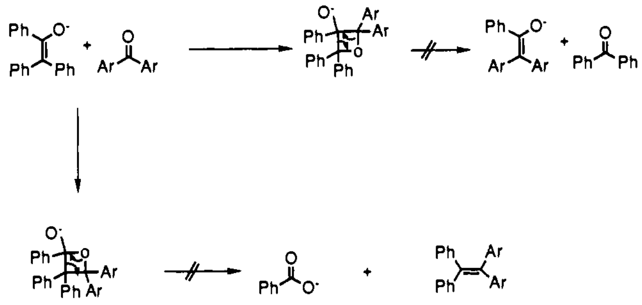

to BP* have been reported previously to give $BP^{\bullet -}$. From enolate **5**, this transfer is thermodynamically allowed since the oxidation potential of **5** is approximately −0.47 V vs SCE, while the reduction potential of BP* is $E_{BP^*/BP^{\bullet -}}$ = 1.55 V vs SCE.[40] Attempts to detect solvated electrons (Na^+, e^-_{sol})[41] were unsuccessful on the 5-ns time scale at which the experiments were carried out.

Mechanism for the Production of 6. A possible mechanism for the formation of enol ester **6** in the presence of BP is suggested in Scheme II. Triplet benzophenone, formed by excitation at 300 nm ≤ λ ≤ 350 nm, accepts an electron from the enolate anion **5**, forming the BP ketyl radical anion ($BP^{\bullet -}$) and the radical **7**. This radical is then trapped by BP to give **8**. Cleavage of the α-phenyl C–C bond results in the formation of **6** and a phenyl radical. A likely driving force for this cleavage is the formation of a conjugated C=O ester bond. The phenyl radical then abstracts a hydrogen atom from solvent, producing benzene.

Appreciable concentrations of the phenyl radical do not seem to accumulate since biphenyl (the expected coupling product) is not observed, nor is phenol formed in detectable quantities. It is known that phenyl radicals are captured by O_2 about 10^3 times more readily than by H atoms (from cyclohexane) at the same molar concentration.[42] In this system, however, abstraction of a hydrogen atom is apparently preferred because the solution is essentially devoid of O_2 because of its uptake to produce BP.

The possibility of a formal [2 + 2] cycloaddition (a Paterno/Büchi reaction) shown in Scheme III as a route to **6** was also considered. A reversible head-to-head addition was eliminated by the absence of tetraphenylethylene in the photoproduct mixture formed in the presence of excess benzophenone (Ar = Ph). By adding 4,4′-dimethylbenzophenone, the possibility of a reversible head-to-tail cycloaddition was eliminated as well, since no unlabeled BP could be isolated at 50% conversion of enolate **5**. Moreover, detection of methylated enol ester **6** when the photolysis of 4,4′-dimethylbenzophenone was conducted in the presence of **5** confirmed the intermolecular interaction of a free substituted BP in the pathway to **6**, as would be consistent with Scheme II.

Scheme IV. Alternate Route for the Formation of **6** via Phenylbenzoate

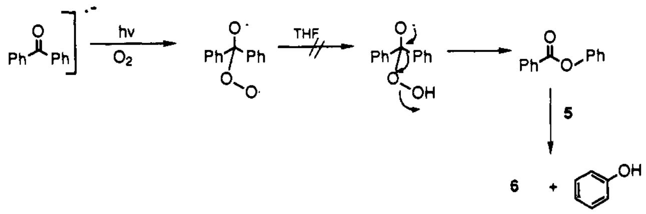

Since partial transesterification of phenyl benzoate is induced by treatment with **5**, Scheme IV, a third possible alternative for the formation of **6** (via a Baeyer–Villiger type rearrangement of an O_2 adduct of $BP^{\bullet -}$) was considered. However, a photoexcitation of an aerated solution of BP is known to not produce measurable quantities of phenylbenzoate.[43] Furthermore, the absence of phenol and phenylbenzoate in the anion reaction mixtures likewise make this mechanism unlikely.

Rationale for the Failed Electrocyclization. Clearly, the altered electron density caused by deprotonation of a ketone to its enolate can cause suppression of the photofragmentation seen in the neutral molecule. The general failure of the trienolate cyclization was unexpected, however. In a previous investigation of stilbene derivatives,[44] failure to photocyclize correlated with enhanced intersystem crossing in a lowest n,π* excited-singlet state. From this excited state, both efficient intersystem crossing ($S^1 \rightarrow T^1$) and internal conversion ($S^1 \rightarrow S^0$) lead to a rapid depopulation of the S^1 level from which photocyclization was believed to proceed. Furthermore, Schaefer and Brauman[8] have shown that enolate anions possess a very low-lying Rydberg-like excited state. Likewise the enolate anions (**2**–**5**) may have an additional low-lying excited state not present in the neutral ketone. From this state, the rapid dissipation of excitation energy would prevent cyclization.[44] Such an energetically low-lying state would also account for the inefficient fluorescence in **4** and **5** and for the contrasting cyclization observed in the enolacetates derived from **5**,[13] where such a low-lying transition would be absent.

If this low-lying state interferes with pericyclic reactivity, the cyclization described by White et al.[9] for **1** would seem to be exceptional. The possibility remains that the cyclization of **1** might be not a photoinduced cyclization but rather a thermal process induced by an initial photochemical geometrical isomerization. This would be consistent with (but obviously not required by) the reactivity reported here for **4** and **5**. The observation of cyclization of **1**, in contrast to the geometrical twisting observed in **2**–**5**, would then relate to product stability and the minimal steric strain encountered in the thermal cyclization of the cis isomer of enolate **1**. Alternatively, unique thermodynamic factors influencing the ring closure of **1** may control its unusual photoreactivity.

Conclusions

Photochemical carbocyclizations of anions **2**–**5** fail, presumably because of the kinetically enhanced depopulation of the S^1 state, facile geometric isomerization, and steric hindrance to thermal cyclization in the disfavored *E*-anions.

Anions **4** and **5** showed broad, red-shifted absorption bands in which the magnitude of the bathochromic shift increases with the associated carbon radius. The oxidation of **4** occurs at less negative potentials than **5**, as is expected from the more extensive delocalization in the more planar anion.

In THF, anion **4** exists in the ground state in solution predominantly as a planar *Z*-isomer, whereas in the solid state it apparently exists as a mixture of *E*- and *Z*-isomers. Photolysis of **4** leads to no stable photoproducts but rather to a bleaching assigned to a reversible geometrical isomerization.

---

(38) Carter, H. V.; McClelland, B. J.; Warhurst, E. *Trans. Faraday Soc.* **1960**, *56*, 455.

(39) Eriksen, J. In *Photoinduced Electron Transfer*; Fox, M. A., Chanon, M., Eds.; Elsevier: Amsterdam, 1988; Part A, p 391.

(40) Chanon, M.; Eberson, L. In *Photoinduced Electron Transfer*; Fox, M. A., Chanon, M., Eds.; Elsevier: Amsterdam, 1988, Part A, p 476.

(41) Bockrath, B.; Dorfman, L. M. *J. Phys. Chem.* **1973**, *77*, 1002.

(42) Russell, G. A.; Bridger, R. F. *J. Am. Chem. Soc.* **1963**, *85*, 3765.

(43) Schwartz, J. Stanford University, Ph.D. Dissertation, 1970.

(44) Blackburn, E. V.; Timmons, C. J. *J. Chem. Soc* (*C*) **1970**, 172.

Anion **5** is locked into a twisted geometry in the ground state with the phenyl groups held at an appreciable angle from the enolate molecular plane. In partially aerated solutions of THF, **5** is converted to **6**, probably through electron transfer from **5** to the benzophenone triplet. Trapping of the oxidized radical by BP and the subsequent cleavage of a phenyl radical completes the proposed conversion.

Experimental Section

Instrumentation. Emission/excitation spectra were recorded on a SLM-AMINCO SPF-500C spectrofluorimeter and absorption spectra were measured on a HP 8451A diode array spectrophotometer. Steady state irradiations were conducted in a Rayonet photochemical reactor (Southern New England Ultraviolet) equipped with low pressure Hg lamps blazed at 300 or 350 nm. For the wavelength dependent photolyses, a 400-nm cut-off filter with a 450-W medium pressure lamp was used. Gas-liquid chromatographic (GC) analyses were obtained on a Hewlett-Packard 5890A instrument equipped with a flame ionization detector and a 0.5 mm × 10 m DB-5 capillary column. ^{1}H and ^{13}C NMR spectra were recorded on a General Electric QE-300 or GN-500 spectrometer. Chemical shifts (δ) are in parts per million (ppm) relative to TMS. ^{13}C CP/MAS spectra were obtained on a Chemagnetics, Inc. CMX-300 spectrometer. Thin-layer chromatography was performed on plastic sheets precoated with silica gel (Macherey-Nagel Polygram, SIL G/UV$_{254}$) visualized under UV light. Flash column chromatography was carried out on MN-Kieselgel 60 silica gel. Cyclic voltammetry was performed with a BAS-100 electrochemical analyzer and a Houston Instruments DMP40 digital plotter.

Solvents and Materials. Tetrahydrofuran (THF, Mallinckrodt, analytical grade) was distilled under nitrogen immediately before use from sodium benzophenone ketyl or molten potassium. Diisopropylamine was distilled prior to use. Tetra-*n*-butylammonium fluorophosphate (Southwestern Analytical, electrochemical grade) was recrystallized from EtOH and dried under vacuum. Sodium hydride (80% in mineral oil), *n*-BuLi (1.6 M), hexamethylphosphoramide (99%, distilled), methyl iodide (99.5%), ferrocene (98%), D_2O (Norell, 99.8% D), acetone-d_6, and THF-d_8 (99.5%) were used as received from Aldrich without further purification. Deoxybenzoin (Aldrich, 97%) was recrystallized twice from 95% EtOH. α,α-Diphenylacetophenone was prepared by the procedure described by Zook et al.[45]

Generation of Sodium Enolate of β-Ionone (2). A mineral oil suspension of NaH (80%, 0.045 g, 1.5 mmol) was placed in a dry 25-mL flask under N_2, rinsed with several small portions of hexane, and suspended in THF (5 mL). To this suspension, β-ionone (0.20 mL, 1 mmol) in THF (5 mL) was added dropwise. The resulting mixture was stirred at room temperature for 2 h, at which time had turned bright yellow-orange. After diluting the reaction mixture with 25 mL of THF, excess D_2O (1 mL) was added, and the resulting solution was stirred for an additional 4 h before quenching with water (10 mL). The aqueous layer was washed with ether, and the combined ether extracts were washed with 5% HCl, water, and brine before being dried over anhydrous $MgSO_4$. After removal of solvent, the residue was examined by ^{1}H NMR (300 MHz, $CDCl_3$) spectroscopy. The peak at 2.25 ppm corresponding to the α-H atoms of **2** had decreased in intensity, indicating 89% deuteration at that site.

Generation of Sodium Enolate of Benzalacetone (3). Anion **3** was generated in a similar manner as above, by treating 0.14 g (1 mmol) of benzalacetone with 0.03 g (1 mmol) of NaH. After D_2O was added, the reaction mixture was stirred for 15 min before quenching with water and workup. After removal of solvent, the residue was examined by ^{1}H NMR (300 MHz, $CDCl_3$) spectroscopy. The peak at 2.38 ppm corresponding to the α-H atoms of **3** had decreased in intensity indicating 66% deuteration at that site.

Generation of Deoxybenzoin Sodium Enolate (4). A mineral oil suspension of NaH (80%, 0.060 g, 2.0 mmol) was placed in a dry 25-mL flask under N_2, rinsed with several small portions of hexane, and suspended in THF (5 mL). The flask was cooled to 0 °C, and 0.20 g (1 mmol) of deoxybenzoin in THF (5 mL) was added dropwise. The resulting mixture was stirred at 0 °C (30 min), warmed to room temperature, and stirred for another 15 min, at which time the reaction mixture had turned bright yellow. MeI (0.31 mL, 5 mmol) was added, and the resulting solution stirred for an additional 30 min. The reaction mixture was then diluted with ether (25 mL) and quenched with cold water (20 mL). The aqueous layer was washed with ether, and the combined ether extracts were washed with 5% HCl, water, and brine before being dried over anhydrous $MgSO_4$. Separation by flash chromatography (5% EtOAc/hexane) gave 71% of the monomethylated product[46] and 27% of the dimethylated product[47] in 0.30 g of combined yield.

Generation of α,α-Diphenylacetophenone Sodium Enolate (5). A mineral oil suspension of NaH (80%, 0.030 g, 1 mmol) was placed in a dry 25-mL flask under N_2, rinsed with several small portions of pentane, and suspended in THF (5 mL). α,α-Diphenylacetophenone (0.14 g, 0.5 mmol) in THF (5 mL) was added dropwise, and the resulting mixture stirred at room temperature for 1 h, at which time the reaction mixture had turned bright yellow. To this solution was added 0.16 mL (2.5 mmol) of MeI, and the resulting mixture was stirred at room temperature for 6 h. The reaction mixture was then diluted with 15 mL of ether and quenched with 2 mL of cold water before being poured into cold water (20 mL). The layers were separated, and the aqueous layer was washed again with ether. The combined ether extracts were washed with 5% HCl, water, and brine before being dried over anhydrous $MgSO_4$. After removal of solvent the residue was subjected to flash chromatography (3/8 CH_2Cl_2/pentane) to isolate 27% of C-methylation product[46] and 71% of O-methylation product[48] in 75% yield.

Solution NMR Studies of 4 and 5. Sodium enolate anions were generated in THF-d_8 as above and were filtered through a fritted glass funnel connected to an NMR tube. The tube containing the filtrate was then sealed under vacuum. Samples prepared this way can be stored indefinitely at low temperature without decomposition. Assignments are based on ^{1}H–^{13}C heteronuclear 2D COSY spectra and literature data[21,49] (for numbering see Figure 3).

4: ^{1}H NMR (500 MHz, THF-d_8) δ 5.6 (s, 1 H, H_e), 6.7 (t, J = 7 Hz, 1 H, H_d), 7.1 (2 t, J = 7 Hz, 3 H, H_e), 7.2 (t, J = 7 Hz, 2 H, H_b), 7.8 (d, J = 7 Hz, 4 H, H_a); ^{13}C NMR (500 MHz, C_4D_8O) δ 93.9 (C_J), 120.4 (C_I), 125.5 (C_H), 126.4 (C-G), 126.5 (C_F), 127.9 (C_E), 128.4 (C_D), 145.1 (C_C), 148.3 (C_B), 167.3 (C_A).

5: ^{1}H NMR (500 MHz, THF-d_8) δ 6.7 (m, 2 H), 6.8 (m, 3 H), 6.9 (t, J = 8 Hz, 2 H), 7.0 (t, J = 8 Hz, 2 H), 7.2 (d, J = 8 Hz, 2 H), 7.4 (t, J = 8 Hz, 1 H), 7.5 (d, J = 8 Hz, 1 H), 7.6 (d, J = 8 Hz, 1 H), 7.7 (d, J = 8 Hz, 1 H); ^{13}C NMR (500 MHz, THF-d_8) δ 107.8, 121.7, 123.2, 125.7, 127.5, 127.7, 127.9, 129.0, 129.1, 129.3, 130.1, 130.6, 132.9, 133.9, 148.1, 148.3, 149.9, 168.1.

Solid State NMR Studies of 4 and 5. The anions generated as above were filtered through a fritted glass funnel to a flask connected to a vacuum line (0.005 mmHg). The flask was opened to the line, and the solvent was removed. The residue was then transferred to a glove bag kept under dry N_2, and the solid salts were ground and packed into NMR tubes. A ^{13}C CP/MAS spectrum was recorded immediately upon preparing the samples. Anions **4** and **5** in the solid state are respectively bright yellow and orange amorphous powders. The solution phase and solid phase NMR spectra of anions **4** and **5** are included in the supplementary material.

Generation of Lithium Enolates of 4 and 5. Under dry Ar, to a solution of freshly distilled diisopropylamine (0.14 mL, 1 mmol) in THF (3 mL) was added 0.63 mL (1 mmol) of a 1.6 M hexane solution of *n*-BuLi at 0 °C. To the resulting mixture, having been stirred for 30 min, was added the corresponding ketone (0.5 mmol) in THF (5 mL). Stirring was continued for an additional 45 min at 0 °C, at which time an intense yellow color indicative of the presence of anion had developed. Excess D_2O (0.1 mL) was added, and the reaction mixture was stirred at room temperature for 2–6 h. The resulting solution was poured onto water overlaid with ether. The ether layer was washed several times with water and brine before being dried over anhydrous $MgSO_4$. After removal of solvent, the residue was examined by ^{1}H NMR (300 MHz, $CDCl_3$) spectroscopy. The peaks at 4.28 ppm and 6.03 ppm corresponding to the α-H atoms of **4** and **5**, respectively, had decreased in intensity, indicating 83% and 82% deuteration at those sites.

Generation of Free Anions. The free anions were generated by adding a few drops of HMPA to the corresponding sodium enolate prepared as above. The presence of the free anion was indicated by an instantaneous increase in color intensity and a red-shift in the absorption spectrum.

Absorption and Emission Spectra. Spectroscopic cells were dried at 130 °C overnight, cooled in a desiccator, flushed with a dry stream of Ar, and maintained under a positive Ar pressure throughout the measurements by capping under an Ar-filled balloon. The anion solution was transferred to the cell via cannula and was diluted with dry, degassed THF. Measurements were made immediately upon preparing the sample.

Cyclic Voltammetry. Measurements were made in a dry box in Ar-saturated THF at 25 °C containing approximately 1 mM anion and 0.3

---

[45] Zook, H. D.; Russo, T. J.; Ferrand, E. F.; Stotz, D. S. *J. Org. Chem.* **1968**, *33*, 2222.

[46] Borowitz, I. J.; Casper, E. W. R.; Crouch, R. K.; Yee, K. C. *J. Org. Chem.* **1972**, *37*, 3873.

[47] Artaud, I.; Torossian, G.; Viout, P. *Tetrahedron* **1985**, *41*, 5031.

[48] Cariou, M. *Bull. Soc. Chim. Fr.* **1988**, *6*, 1015.

[49] Vogt, H.-H.; Gompper, R. *Chem. Ber.* **1981**, *114*, 2884.

M tetra-*n*-butylammonium hexafluorophosphate as supporting electrolyte. The electrochemical cell was a single cell composed of a Ag/AgCl reference electrode, a Pt flag (0.78 cm^2) as counter electrode, and a Pt disk working electrode. The internal standard (ferrocene/ferrocenium) was added after the first cyclic voltammetric measurement was completed. The Cp_2Fe/Cp_2Fe^+ couple under these conditions was found to be 0.55 V vs Ag/AgCl.

Enol Acetate of Deoxybenzoin. A mineral oil suspension of NaH (60%, 0.12 g, 3 mmol) was placed in a dry 50-mL flask under N_2, washed with hexane, and suspended in 10 mL of THF. The flask was cooled to 0 °C before 0.39 g (2 mmol) of deoxybenzoin in THF (10 mL) was added. The resulting solution was warmed to room temperature and stirred for 3 h. To this solution was added 1 mL (10 mmol) of acetic anhydride at 0 °C. The mixture was warmed to room temperature and stirred for an additional 3 h before being poured onto water overlaid with ether. The water layer was extracted with ether, and the combined ether extracts were washed sequentially with water and brine, dried over $MgSO_4$, and evaporated to dryness. The crude product was purified by flash chromatography (7:3 pentane/CH_2Cl_2) to give the *Z*-enol acetate as a white solid in 97% yield, identical in every respect with an authentic sample.[24]

Molecular Orbital Calculations. Calculations employed the standard[26] version of AM-1 as implemented in the AMPAC[50] package of computer programs. All bond lengths and angles were optimized with respect to all geometrical parameters, without making any assumptions. The transition state was located by the reaction coordinate method,[51] optimized by minimizing the scalar gradient of the energy,[52,53] and characterized by calculating the force constant. Calculated charge densities of anions **4** and **5** are included in the supplementary material.

Steady State Photolyses. The sodium enolate anions, prepared as described above, were transferred to a Pyrex photocell via canula under a positive N_2 pressure and were diluted with dry THF to give a 0.001 M solution. The resulting solutions were irradiated with 16 low pressure mercury lamps blazed at 350 nm in a Rayonet photochemical reactor while stirring and cooling with chilled water to a reaction temperature consistently below room temperature.

For anion **2** irradiations were done at a series of different temperatures using a cold finger (room temperature, 0 °C, −17 °C, and −60 °C) and base concentrations (0.5, 1, 1.5 equiv). After a measured irradiation period, the reaction mixture was quenched with 5% HCl, extracted to ether and washed sequentially with 5% $NaHCO_3$, water, and brine before being dried over anhydrous $MgSO_4$. Two products were isolated by flash chromatography (CH_2Cl_2/pentane, 3:7 and then 7:3): α-pyran[54] (64%, irradiation at 0 °C) and (*Z*)-*retro*-γ-ionone[11] (9%, irradiation at 0 °C). No other products were detected.

After 2 h of irradiating anion **3**, the reaction mixture was quenched with 5% HCl extracted to ether and washed sequentially with 5% $NaHCO_3$, water, and brine before being dried over anhydrous $MgSO_4$. Separation by flash chromatography (CH_2Cl_2) gave *Z*-**3**[55] in 63% yield.

Anion **4** was irradiated up for periods ranging to 10 h, after which the reaction mixture was quenched with 5% HCl and washed sequentially with 5% $NaHCO_3$, water, and brine before being dried over anhydrous $MgSO_4$. The reaction mixture analyzed by GC showed the presence of starting material only.

For anion **5**, after a measured irradiation period (4 h), the reaction mixture was quenched with 5% HCl, extracted with ether, and washed sequentially with 5% $NaHCO_3$, water, and brine before being dried over anhydrous $MgSO_4$. Analysis of the reaction mixture by GC gave 37% of **6**, ca. 25% benzene, and 17% of BP, based on starting material consumption. Solvent was removed under vacuum and was collected in a liquid N_2 trap. The residue was warmed to room temperature, and the THF was distilled through a Vigreaux column (66–68 °C) by maintaining a water bath at 75 °C until about 5 mL of solvent remained. Analysis of the residue by UV, GC, MS, and HRMS showed the presence of benzene but no phenol or biphenyl.

The enol ester **6** was separated by flash chromatography, first with benzene/pentane (6:4) and then with benzene/C_6H_{12} (3:1). Recrystallization from methanol by slow evaporation at room temperature gave **6** as fine, white colorless needles, mp 147–149 °C. The structure of **6** was solved by X-ray analysis; the data were collected at room temperature on a Nicolet R3 diffractometer using a graphite monochromator and Mo Kα radiation (λ = 0.7107 Å). The crystal system is monoclinic, and the space group is $P2_1/c$; a = 9.054 (6) Å, b = 5.623 (3) Å, c = 40.23 (6) Å; β = 90.846 (10)°, V = 2048 (4) Å^3, ρ_{calc} = 1.22 gcm^3 for Z = 4, F(000) = 792. Complete data are included as supplementary material.

For dark control reactions, a cell prepared identically as the photolyses mixture was covered with aluminum foil while all other experimental conditions were kept constant. The rate of appearance of benzophenone, as monitored by GC, in this dark control was equivalent to the rate of appearance of BP and **6** in the photolysis mixture.

Suppression of the Formation of 6 in the Absence of Oxygen. To a 1-in. ID Pyrex tube equipped with two side arms and a glass tube adaptor for a vacuum connection was added a solution of α,α'-diphenylacetophenone (0.068 g, 0.25 mmol) in THF (50 mL). Oil free NaH (0.015 g, 0.5 mmol) was placed in one side arm. The THF solution was degassed by a freeze–pump–thaw cycle process at least 4 times before being sealed. When the solution had warmed to room temperature, the solution was mixed with the NaH in the side arm, and the resulting mixture was stirred for 2 h. Analysis of the reaction mixture after photolysis (4 h) and workup showed the presence of the starting ketone only.

Effect of BP on the Formation of 6. To the same apparatus was added oil free NaH (0.015 g, 0.5 mmol) in one side arm and BP (0.045 g, 0.25 mmol) in the other. The ketone (0.068 g, 0.25 mmol) in THF (50 mL) contained in the Pyrex tube was degassed by a freeze–pump–thaw cycle process at least 4 times, and the reaction vessel was sealed off. The anion was generated by adding the NaH and stirring at room temperature for 2 h. Before irradiating the reaction mixture (3 h), BP contained in the other side arm was added. Analysis of the reaction mixture after workup showed formation of **6** in 10% yield.[32]

This experiment was repeated by adding oil free NaH (0.015 g, 0.5 mmol) in one side arm and 4,4′-dimethylbenzophenone (0.052 g, 0.25 mmol) in the other. The ketone (0.068 g, 0.25 mmol) in THF (50 mL) contained in the Pyrex tube was degassed, and the reaction vessel was sealed off. After generating the anion (2 h), 4,4′-dimethylbenzophenone in the side arm was added, and the reaction mixture was irradiated (3 h). Analysis of the reaction mixture, after workup by GC, showed no (<1%) unlabeled BP present. Separation by flash chromatography (benzene) gave the *p*-Me phenylester derivative of **6**[32] in 15% yield: ^{1}H NMR (500 MHz, acetone-d_6) δ 3.8 (s, 3 H), 7.2 (m, 19 H); MS (FAB) *m/z* 391 (8%, M).

Wavelength Dependence in the Steady State Photolysis of 5. A solution of anion **5** as sodium enolate, prepared as above, was irradiated using a 450-W medium pressure lamp through a 400-nm cut-off filter window. No enol ester product **6** was detected even after 8 h of irradiation. Another solution of **5** irradiated through a Pyrex filter (>300 nm) under identical conditions gave **6** in 19% yield after 1.5 h based on starting material consumption.

Fast Kinetics Experiments. Flash photolyses experiments were performed on a frequency doubled Q-switched Nd:YAG laser (Quantel YG 481, 8 ns pulse, approximately 100 mJ at 355 nm), with a pulse-to-pulse reproducibility better than 10%. Transient absorptions were monitored with a conventional xenon lamp, monochromator, photomultiplier arrangement. All decay traces were an average of 20 pulses and are corrected for background. The samples were stirred after at least every five shots.

Acknowledgment. This research was supported by the National Science Foundation and the Robert A. Welch Foundation. The flash photolyses studies were conducted at the Center for Fast Kinetics Research which is supported jointly by the Biotechnology Resources Program of the Division of Research Resources of NIH (RR 00886) and by the University of Texas at Austin. We are grateful to Dr. Anthony Harriman for help with the flash photolyses, Dr. Yu-Jun Zheng for assistance with the MO calculations, Dr. Vincent Lynch for carrying out the X-ray analysis, and Dr. Ben Shoulders for helpful discussions of the NMR data.

Supplementary Material Available: Solution phase ^{1}H and ^{13}C NMR, APT, ^{1}H-^{13}C heteronuclear 2D COSY spectra, and solid state ^{13}C CP/MAS spectra, AM-1 calculated charge densities of **4** and **5**, X-ray analysis of **6**, and tables of isotropic and anisotropic thermal parameters, bond lengths and angles, and torsion angles, atom labeling scheme, and unit cell packing diagram for $C_{27}H_{20}O_2$ (22 pages); table of observed and calculated structure factors (10 pages). Ordering information is given on any current masthead page.

---

(50) QCPE Publication 506, Department of Chemistry, Indiana University, Bloomington, IN 47405. An improved version (AMPAC 2.1) is now available.

(51) Dewar, M. J. S.; Kirschner, S. *J. Am. Chem. Soc.* **1971**, *93*, 4290.

(52) McIver, J. W.; Komornicki, J. *Chem. Phys. Lett.* **1971**, *10*, 303.

(53) McIver, J. W.; Komornicki, J. *J. Am. Chem. Soc.* **1972**, *94*, 2625.

(54) Marvell, E. N.; Caple, G.; Gosink, T. A.; Zimmer, G. *J. Am. Chem. Soc.* **1966**, *88*, 619.

(55) Baas, P.; Cerfontain, H. *Tetrahedron* **1977**, *33*, 1509.